



Adsorption properties and inhibition of carbon steel corrosion in hydrochloric acid solution by Ethyl 3-hydroxy-8-methyl-4-oxo-6-phenyl-2-(p-toly)-4,6-dihydropyrimido[2,1-b] [1,3]thiazine-7-carboxylate

M. Larouj^a, H. Lgaz^a, H. Serrar^d, H. Zarrok^a, H. Bourazmi^b, A. Zarrouk^c,
A. Elmidaoui^a, A. Guenbour^b, S. Boukhris^d and H. Oudda^a

^aLaboratory of Separation Processes, Central Post 133, Kenitra, Faculty of Sciences, University IbnTofail, Morocco.

^bLaboratory of Nanotechnology, Materials, and Environment Faculty of Sciences, Rabat, Morocco.

^cURAC18, Faculty of Sciences, University Mohammed one, Oujda, Morocco.

^dLaboratory of Organic Synthesis, Organometallic and theoretical, Faculty of Sciences, University IbnTofail, Kenitra, Morocco

Received 24 Apr 2015, Revised 23 Nov 2015, Accepted 29 Nov 2015

* Corresponding Author: Email: ouddahassan@gmail.com ;

Abstract

Ethyl 3-hydroxy-8-methyl-4-oxo-6-phenyl-2-(p-toly)-4,6-dihydropyrimido[2,1-b] [1,3]thiazine-7-carboxylate. (PT) was examined as a corrosion inhibitor for carbon steel in 1.0 M HCl by using electrochemical impedance spectroscopy (EIS) and potentiodynamic polarization (PDP). Results show that PT is a good inhibitor and its inhibition efficiency reaches 95 % at 10^{-3} M. The percentage inhibition efficiency (η) was found to increase with increase of the inhibitor concentration due to the adsorption of the inhibitor molecules on the metal surface. Tafel polarisation study revealed that (PT) acts as a mixed type inhibitor. In addition it was established the adsorption follows Langmuir adsorption isotherm. Moreover, the thermodynamic activation parameters for the corrosion reaction were calculated and discussed in relation to the stability of the protective inhibitor layer. Quantum chemical parameters are calculated using the Density Functional Theory method (DFT). Correlation between theoretical and experimental results is discussed.

Key words: Carbon steel; Hydrochloric acid; Corrosion inhibition; Adsorption; pyrimidothiazine derivative.

1. Introduction

The protection of metal surfaces against corrosion is an important industrial and scientific topic. Inhibitors are one of the practical means of preventing corrosion, particularly in acidic media. Inhibitors can adhere to a metal surface to form a protective barrier against corrosive agents in contact with metal. The effectiveness of an inhibitor to provide corrosion protection depends to large extent upon the interaction between the inhibitor and the metal surface. The adsorbed inhibitors can affect the corrosion reaction either by the blocking effect of adsorbed inhibitor on the metal surface or by the effects attributed to the change in the activation barriers of the anodic and cathodic reactions of the corrosion process.

Organic compounds which can donate electrons to unoccupied d orbitals of metal surface to form coordinate covalent bonds and can also accept free electrons from the metal surface by using their antibond orbitals to form feedback bonds constitute excellent corrosion inhibitors. Researchers conclude that the adsorption on the metal surface depends mainly on the physicochemical properties of the inhibitor group, such as the functional group, electronic density at the donor atom, p orbital character [1-22]. The molecular electronic structure with number of adsorption active centers such as S, N and O atoms, the molecular size, the mode of adsorption, the formation of metallic complexes and the projected area of the inhibitor on the metallic surface (degree of surface coverage) also affect the efficiency of inhibition.

The choice of an appropriate inhibitor depends on the physicochemical properties of the inhibitor molecule, the nature and state of the metal surface, and the type of the corrosion medium. Inhibitors have been selected mainly by using empirical knowledge based on their macroscopic physicochemical properties. Recently, the effectiveness of an inhibitor molecule has been related to its spatial as well as its electronic structure [23-26].

2. Experimental details

2.1. Materials

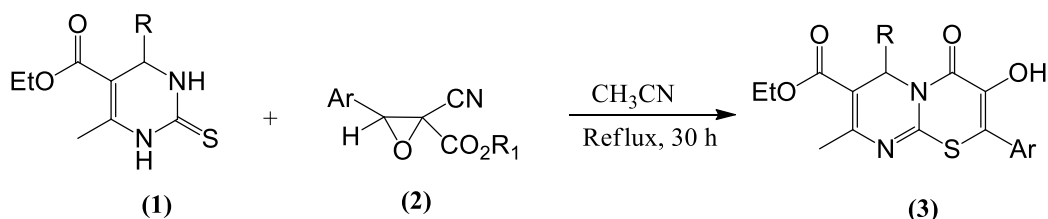
The steel used in this study is a carbon steel (Euronorm: C35E carbon steel and US specification: SAE 1035) with a chemical composition (in wt%) of 0.370 % C, 0.230 % Si, 0.680 % Mn, 0.016 % S, 0.077 % Cr, 0.011 % Ti, 0.059 % Ni, 0.009 % Co, 0.160 % Cu and the remainder iron (Fe). The carbon steel samples were pre-treated prior to the experiments by grinding with emery paper SiC (120, 600 and 1200); rinsed with distilled water, degreased in acetone in an ultrasonic bath immersion for 5 min, washed again with bidistilled water and then dried at room temperature before use.

2.2. Solutions

The aggressive solutions of 1.0 M HCl were prepared by dilution of analytical grade 37% HCl with distilled water. The concentration range of Ethyl 3-hydroxy-8-methyl-4-oxo-6-phenyl-2-(p-toly)-4,6-dihydropyrimido[2,1-b][1,3]thiazine-7-carboxylate used was 1×10^{-6} M to 1×10^{-3} M.

2.3. Synthesis

General procedure for the Synthesis of ethyl 3-hydroxy-8-methyl-4-oxo-4,6-dihydropyrimido[2,1-b][1,3]thiazine-7-carboxylate :



To a solution of epoxide (2) (1 mmol) in acetonitrile (20 ml), ethyl 6-methyl-4-aryl-2-thioxo-1,2,3,4-tetrahydropyrimidine-5-carboxylate (1) (1mmol) was added, and the mixture was refluxed for 3h. The reaction mixture was distilled using rotary vacuum evaporator to afford crude product, which was treated with a mixture of ether/petroleum ether, the 3-hydroxy-4,6-dioxo-pyrimido[2,1-b][1,3]thiazine-7-carbonitriles (3) . [27]

2.4. Corrosion tests

2.4.1. Electrochemical impedance spectroscopy

The electrochemical measurements were carried out using Volta lab (Tacussel- Radiometer PGZ 100) potentiostat and controlled by Tacussel corrosion analysis software model (Volta master 4) at under static condition. The corrosion cell used had three electrodes. The reference electrode was a saturated calomel electrode (SCE). A platinum electrode was used as auxiliary electrode of surface area of 1 cm². The working electrode was carbon steel. All potentials given in this study were referred to this reference electrode. The working electrode was immersed in test solution for 30 minutes to establish steady state open circuit potential (E_{ocp}). After measuring the E_{ocp}, the electrochemical measurements were performed. All electrochemical tests have been performed in aerated solutions at 303 K. The EIS experiments were conducted in the frequency range with high limit of 100 kHz and different low limit 100 mHz at open circuit potential, with 10 points per decade, at the rest potential, after 30 min of acid immersion, by applying 10 mV ac voltage peak-to-peak. Nyquist plots were made from these experiments. The best semicircle can be fit through the data points in the Nyquist plot using a non-linear least square fit so as to give the intersections with the x-axis.

2.4.2. Potentiodynamic polarization

The electrochemical behaviour of carbon steel sample in inhibited and uninhibited solution was studied by recording anodic and cathodic potentiodynamic polarization curves. Measurements were performed in the 1.0 M HCl solution containing different concentrations of the tested inhibitor by changing the electrode potential automatically from - 800 to -100 mV versus corrosion potential at a scan rate of 2 mV.s⁻¹. The linear Tafel segments of anodic and cathodic curves were extrapolated to corrosion potential to obtain corrosion current densities (I_{corr}).

The present investigation was undertaken to examine the corrosion inhibition capacity of a Ethyl 3-hydroxy-8-methyl-4-oxo-6-phenyl-2-(p-toly)-4,6-dihydropyrimido[2,1-b] [1,3]thiazine-7-carboxylate. in 1.0 M HCl solution on carbon steel at 303-333 K using potentiodynamic polarisation (PDP) curves and electrochemical impedance spectroscopy (EIS) methods. The adsorption isotherm of inhibitor on steel surface was determined. Kinetic parameters are calculated and discussed in detail. Figure 1 shows the molecular structure of the pyrimidothiazine derivative utilised in this investigation.

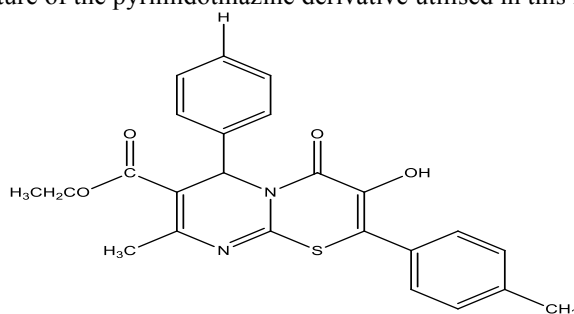


Figure 1: Chemical structure of Ethyl 3-hydroxy-8-methyl-4-oxo-6-phenyl-2-(p-toly)-4,6-dihydropyrimido[2,1-b] [1,3]thiazine-7-carboxylate.

2.4.3. Weight loss measurements

Gravimetric measurements were carried out at definite time interval of 4 h at room temperature using an analytical balance (precision ± 0.1 mg). The carbon steel specimens used have a rectangular form (length = 1.6 cm, width = 1.6 cm, thickness = 0.07 cm). Gravimetric experiments were carried out in a double glass cell equipped with a thermostated cooling condenser containing 80 mL of non-de-aerated test solution. After immersion period, the steel specimens were withdrawn, carefully rinsed with bidistilled water, ultrasonic cleaning in acetone, dried at room temperature and then weighed. Triplicate experiments were performed in each case and the mean value of the weight loss was calculated.

2.4.4. Molecular Modelling

Complete geometrical optimizations of the investigated molecules are performed using DFT (density functional theory) with the Beck's three parameter exchange functional along with the Lee-Yang-Parr nonlocal correlation functional (B₃LYP) with 6-31G* basis set is implemented in Gaussian 03 program package [28-30]. This approach is shown to yield favorable geometries for a wide variety of systems. This basis set gives good geometry optimizations. The geometry structure was optimized under no constraint. The following quantum chemical parameters were calculated from the obtained optimized structure: The highest occupied molecular orbital (E_{HOMO}) and the lowest unoccupied molecular orbital (E_{LUMO}), the energy difference (ΔE) between E_{HOMO} and E_{LUMO} , dipole moment (μ), electron affinity (A), ionization potential (I) and the fraction of electrons transferred (ΔN).

According to Koopman's theorem [32] the ionization potential (IE) and electron affinity (EA) of the inhibitors are calculated using the following equations.

$$IE = -E_{HOMO}$$

$$EA = -E_{LUMO}$$

Thus, the values of the electronegativity (χ) and the chemical hardness (η) according to Pearson, operational and approximate definitions can be evaluated using the following relations [33]:

$$\chi = \frac{IE + EA}{2}$$
$$\eta = \frac{IE - EA}{2}$$

The number of transferred electrons (ΔN) was also calculated depending on the quantum chemical method [34-35] by using the equation:

$$\Delta N = \frac{\chi_{Fe} - \chi_{inh}}{2(\eta_{Fe} + \eta_{inh})}$$

Where χ_{Fe} and χ_{inh} denote the absolute electronegativity of iron and inhibitor molecule η_{Fe} and η_{inh} denote the absolute hardness of iron and the inhibitor molecule respectively. In this study, we use the theoretical value of $\chi_{Fe} = 7.0$ eV and $\eta_{Fe} = 0$, for calculating the number of electron transferred.

3. Results and discussion

3.1. Tafel polarisation study

3.1.1. Effect of PT concentration

Polarization measurements have been carried out in order to gain knowledge concerning the kinetics of the anodic and cathodic reactions. Typical potentiodynamic polarization curves of the carbon steel in 1.0 M HCl solutions without and with addition of different concentrations of (PT) are shown in Fig.2. Electrochemical kinetic parameters (corrosion potential (E_{corr}), corrosion current density (I_{corr}) and cathodic Tafel slope (β_c)), determined from these experiments by extrapolation method [36], are reported in Table 1. The I_{corr} was determined by Tafel extrapolation of only the cathodic polarization curve alone, which usually produces a longer and better defined Tafel region [37]. The I_{corr} values were used to calculate the inhibition efficiency, η_{Tafel} (%), (listed in Table 1), using the following equation [38]:

$$\eta_{Tafel}(\%) = \frac{I_{corr} - I_{corr(i)}}{I_{corr}} \times 100 \quad (1)$$

where I_{corr} and $I_{corr(i)}$ are the corrosion current densities for steel electrode in the uninhibited and inhibited solutions, respectively.

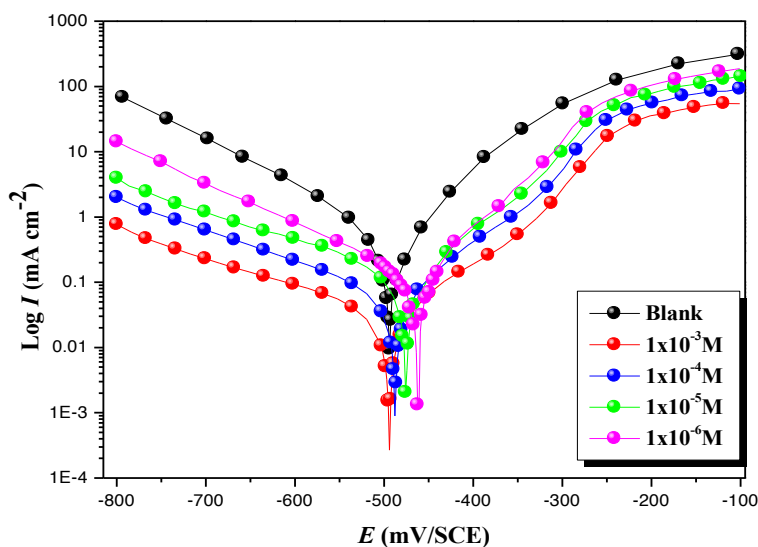


Figure 2: Typical polarisation curves for carbon steel in 1.0 M HCl for various concentrations of (PT) at 303 K

Inspection of the figure 2 shows that the addition of (PT) has an inhibitive effect in the both anodic and cathodic parts of the polarization curves and generally shifted the E_{corr} value towards the negative direction compared to the uninhibited steel. Thus, addition of this inhibitor reduces the carbon steel dissolution as well as retards the hydrogen evolution reaction. In addition, the parallel cathodic Tafel curves in Fig. 2 show that the hydrogen evolution is activation-controlled and the reduction mechanism is not affected by the presence of the inhibitor [39]. So, it could be concluded that this Ethyl 3-hydroxy-8-methyl-4-oxo-6-phenyl-2-(p-toly)-4,6-dihydropyrimido[2,1-b] [1,3]thiazine-7-carboxylate. (PT) is of the mixed-type inhibitor for steel in 1.0 M HCl solution. Indeed, this inhibitor can exist as a

cationic species in 1.0 M HCl medium, which may be adsorbed on the cathodic sites of the carbon steel and reduce the evolution of hydrogen. Moreover, the adsorption of this compound on anodic sites through the lone pairs of electrons of nitrogen, and sulphur atoms will then reduce the anodic dissolution of carbon steel.

The analyse of the data in Table 1 revealed that the corrosion current density (I_{corr}) decreases considerably with increasing (PT) concentration, with a negative shift in corrosion potential compared to that of uninhibited solution. From table we can classify an inhibitor as cathodic or anodic type if the displacement in corrosion potential is more than 85 mV with respect to corrosion potential of the blank [40]. In the presence of this Thiophene derivative, the corrosion potential of carbon steel shifted to the negative side only 33 mV (vs. SCE). This can be interpreted that inhibitor acts as a mixed type inhibitor and shows more pronounced influence in the cathodic polarization plots compared to that in the anodic plots. The values of β_c show a slight change with increasing inhibitor concentration, indicating the influence of the (PT) on the kinetics of hydrogen evolution. This may probably be due to a diffusion or barrier effect [41]. The dependence of $\eta_{Tafel}(\%)$ versus the inhibitor concentration of (PT) is also presented in Table 1. The obtained efficiencies indicate that (PT) acts as effective inhibitor. Indeed, the values of $\eta_{Tafel}(\%)$ increase with inhibitor concentration, reaching its maximum value, 94.5 %, at 1×10^{-3} M.

Table 1: Polarisation parameters and the corresponding inhibition efficiency of carbon steel corrosion in 1.0 M HCl containing different concentrations of (PT) at 303 K.

Inhibitor	Concentration (M)	$-E_{corr}$ vs. SCE (mV)	$-\beta_c$ (mV dec ⁻¹)	I_{corr} ($\mu A\ cm^{-2}$)	η_{Tafel} (%)
Blank	—	496	163	564	—
(PT)	1×10^{-3}	498	195	35.7	94.0
	1×10^{-4}	492	187	63.0	89.0
	1×10^{-5}	478	181	85.5	85.0
	1×10^{-6}	465	163	110	80.5

3.2. Impedance spectroscopy

The corrosion of carbon steel in 1.0 M HCl solution in the presence of (PT) was investigated by EIS at room temperature after an exposure period of 30 min. Nyquist plots for carbon steel obtained at the interface in the absence and presence of this inhibitor at different concentrations is given in Fig. 3.

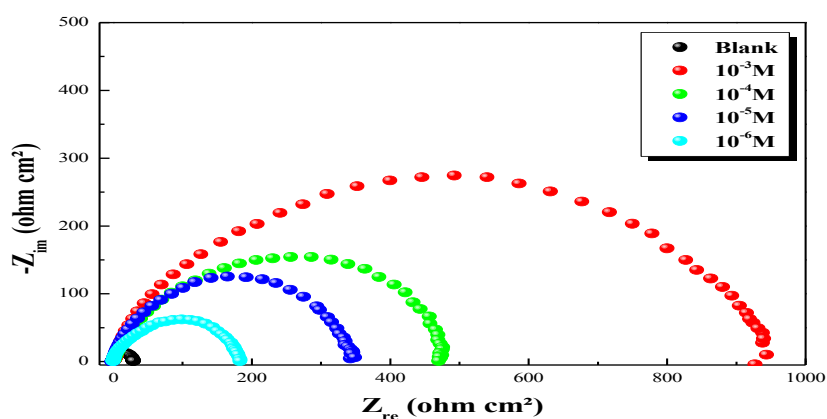


Figure 3: Nyquist plot for carbon steel in 1.0 M HCl solution in presence of (PT).

The impedance diagram obtained with 1.0 M HCl shows only one depressed capacitive loop at the higher frequency range. The same trend was also noticed for carbon steel immersed in 1.0 M HCl containing (PT) (10^{-6} - 10^{-3} M). Table 2 lists impedance parameters of the Nyquist plots of the (PT) in different concentrations. R_{ct} represents the charge-transfer resistance whose value is a measure of electron transfer across the surface and is inversely proportional to

corrosion rate [42]. The constant phase element, CPE (Fig. 4), is introduced in the circuit instead of a pure double layer capacitor to give a more accurate fit [43].

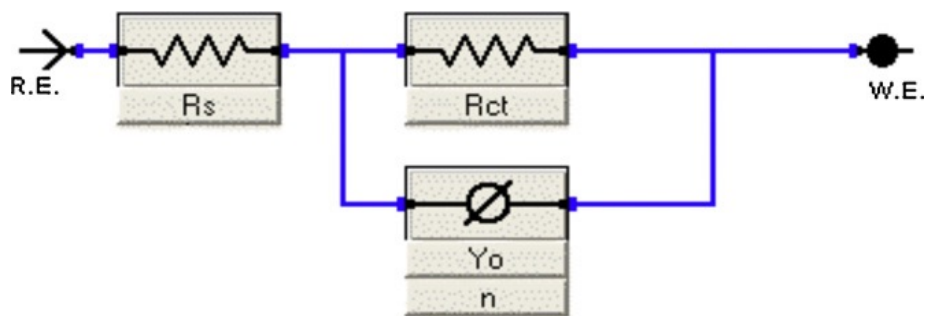


Figure 4: The Randles CPE circuit which is the equivalent circuit for this impedance spectra.

Table 2: AC impedance data of carbon steel in 1.0 M hydrochloric acid solution for (PT) at 303K

Inhibitor	Concentration (M)	R_t ($\Omega \text{ cm}^2$)	$Y_0 \times 10^{-4}$ ($\text{sn } \Omega^{-1} \text{ cm}^{-2}$)	n	C_{dl} ($\mu\text{F/cm}^2$)	η_{EIS} (%)
Blank	—	32.8	1.7618	0.87	97	—
	1×10^{-3}	869.7	0.17797	0.80	6.28	96.2
	1×10^{-4}	463.4	0.26300	0.80	7.23	92.9
(PT)	1×10^{-5}	306.2	0.27589	0.87	13.52	89.3
	1×10^{-6}	174.1	0.64821	0.81	22.64	81.2

The diameter of Nyquist plots increases on increasing the (PT) concentration. This suggested that the formed inhibitive film was strengthened by addition of (PT). The high frequency (HF) loops have depressed semicircular appearance, $0.5 \leq n \leq 1$, which is often referred to as frequency dispersion as a result of the inhomogeneity [44-46] or the roughness [47] of the solid surface. It should be noted that a CPE (Fig. 4) could be treated as a parallel combination of a pure capacitor and a resistor being inversely proportional to the angular frequency. The CPE, which is considered a surface irregularity of the electrode, causes a greater depression in Nyquist semicircle diagram, where the metal-solution interface acts as a capacitor with irregular surface [48]. The impedance of the CPE is expressed as:

$$Z_{\text{CPE}} = \frac{1}{Y_0 (j\omega)^n} \quad (2)$$

Where Y_0 is the magnitude of the CPE, j is the imaginary unit, ω is the angular frequency ($\omega = 2\pi f$, where f is the AC frequency) and n is the CPE exponent (phase shift). The general unit for CPE is in F cm^{-2} (Farad cm^{-2}).

The inhibition efficiency of the inhibitor was calculated from the charge transfer resistance values using the following equation:

$$\eta_z \% = \frac{R_{ct}^i - R_{ct}^\circ}{R_{ct}^i} \times 100 \quad (3)$$

Where, R_{ct}^i and R_{ct}° are the charge transfer resistance in absence and in presence of inhibitor, respectively. The EIS measurement reveals that at the concentration of 10^{-3} M, the percentage of inhibition efficiency is highest (96.2% η_z). The result strongly supports the observation that 10^{-3} M of this compound could work best as an inhibitor. The results also show that R_{ct} values increased with increase in additive concentration except few cases. The percentage inhibition efficiencies calculated from the R_{ct} values indicate that (PT) acts as a good corrosion inhibitor of carbon steel in HCl medium. The CPE values found to decrease with increase in concentration of inhibitor solutions. This behaviour is generally seen for system where inhibition occurred due to the formation of a surface film by the adsorption of inhibitor on the metal surface [49-50]. Decrease in CPE, which can result from a decrease in local dielectric constant and/or an increase in the thickness of the electrical double layer, suggest that the inhibitor molecules

act by adsorption at the metal/solution interface [51]. The values of n obtained for this inhibitor system were close to unity which shows that the interface behaves nearly capacitive [52].

3.3. Weight loss, corrosion rates and inhibition efficiency

The corrosion rate (A) of carbon steel specimens after 4 h exposure to 1.0 M HCl solution with and without the addition of various concentrations of the investigated inhibitor was calculated and the obtained data are listed in Table 3. The variation of A with inhibitor concentrations is shown in Fig. 5. The corrosion rate, A (mg cm⁻² h⁻¹), surface coverage (θ) and inhibition efficiency η_w of each concentration were calculated using the following equations [53]:

$$A = \frac{\Delta W}{St} \tag{4}$$

$$\theta = \frac{A_{uninh} - A_{inh}}{A_{uninh}} \tag{5}$$

$$\eta_w = \left(\frac{A_{uninh} - A_{inh}}{A_{uninh}} \right) \times 100 \tag{6}$$

Where ΔW is the average weight loss (mg), S is the surface area of specimens (cm²), and t is the immersion time (h), A_{uninh} and A_{inh} are corrosion rates in the absence and presence of inhibitor, respectively.

Table 3: Effect of (PT) concentration on corrosion data of carbon steel in 1.0M HCl

Inhibitor	Conc. (M)	A (mg cm ⁻² h ⁻¹)	η _w (%)	(θ)
Blank	1.0	1.125	-	-
(PT)	1×10 ⁻³	0.0412	96.34	0.9634
	1×10 ⁻⁴	0.0931	91.73	0.9173
	1×10 ⁻⁵	0.1324	88.23	0.8823
	1×10 ⁻⁶	0.2029	81.96	0.8196

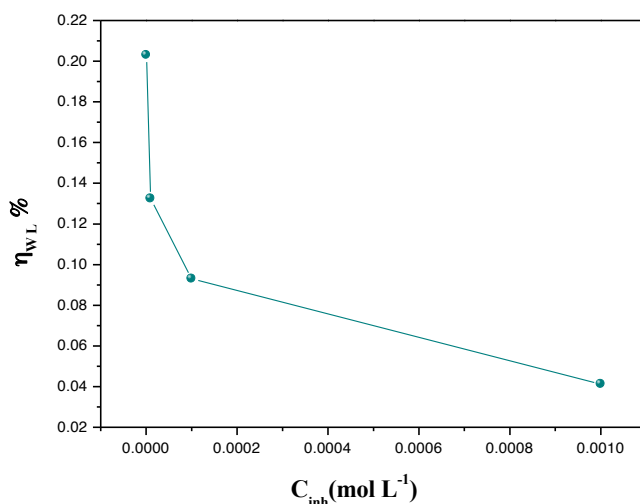


Figure 5. Relationship between the corrosion rate and inhibitor concentration for carbon steel after 4h immersion in 1.0 M HCl at 303K.

It is clear that η_w increased with increasing inhibitor concentration, while corrosion rate decreased. This could be due to the fact that the inhibitor molecules act by adsorption on the metal surface[54].The variation of η_w and inhibitor concentrations in 1.0 M HCl solution at 303 K is shown in Fig 6. The maximum η_w value of (10⁻³ M) of this inhibitor was found.

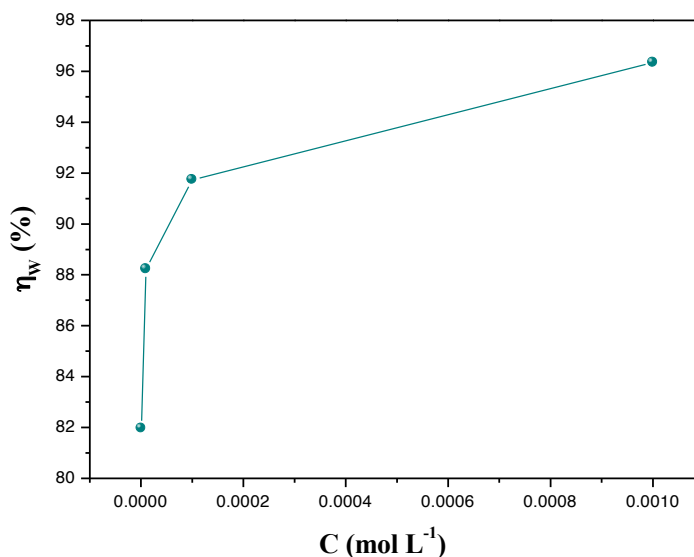


Figure.6. Relationship between the inhibition efficiency and inhibitor concentration for carbon steel after 4 h immersion in 1.0 M HCl at 303K.

3.4. Effect of temperature

The effect of temperature on the inhibited acid–metal reaction is very complex, because many changes occur on the metal surface such as rapid etching, desorption of inhibitor and the inhibitor itself may undergo decomposition [55]. The effect of temperature on the inhibition performance of (PT) for carbon steel in 1.0 M HCl solution in the absence and presence of 1×10^{-3} M concentration at temperature ranging from 303 to 333 K was obtained by potentiodynamic polarization measurements (Figs 5 and 6). The results are given in Table 3.

The inhibition efficiencies are found to decrease with increasing the solution temperature from 303 K to 333 K. This behaviour can be interpreted on the basis that the increase in temperature results in desorption of the inhibitor molecules from the surface of carbon steel. Table 3 shows that the corrosion rate increased with increasing temperature both in uninhibited and inhibited solutions. The corrosion rate increases more rapidly with temperature in the absence of the inhibitor. These results confirm that pyrimidothiazine derivative acts as an efficient inhibitor for carbon steel in 1.0 M HCl in the range of temperature studied.

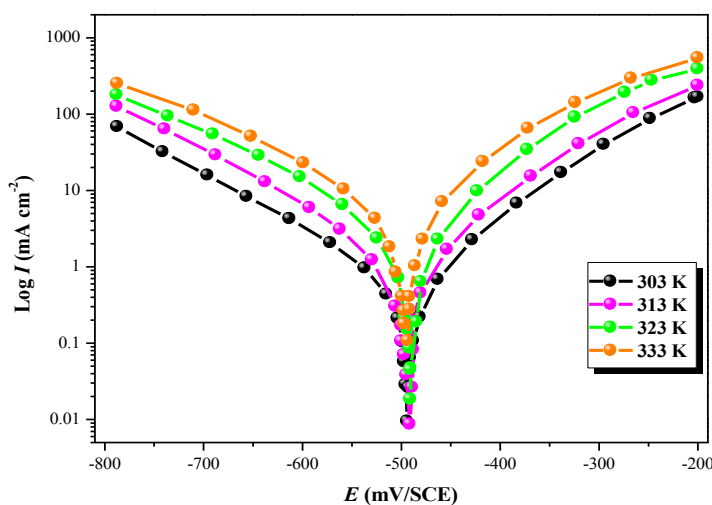


Figure 7: Potentiodynamic polarisation curves of carbon steel in 1.0 M HCl at different temperatures

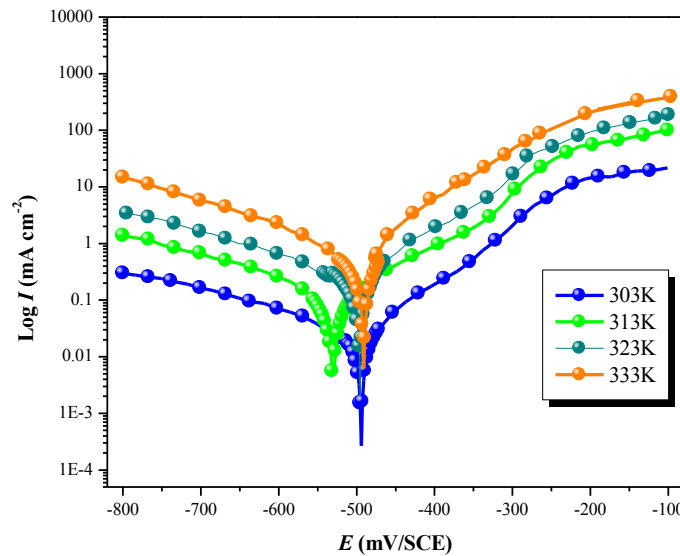


Figure 8: Potentiodynamic polarisation curves of carbon steel in 1.0 M HCl in the presence of the optimum concentration of 1×10^{-3} M (PT) at different temperatures.

Table 4: Electrochemical characteristics of carbon steel in 1.0 M HCl without and with 1×10^{-3} M of the studied inhibitor at different temperatures derived from current-voltage I-E characteristics.

Inhibitor	Temperature K	$-E_{corr}$ vs. SCE(mV)	$-\beta_c$ (mV dec ⁻¹)	i_{corr} (μ A cm ⁻²)	η_{Tafel} (%)
Blank	303	496	163	564	—
	313	498	155	773	—
	323	492	176	1244	—
	333	497	192	1650	—
10^{-3}M (PT)	303	498	195	35.65	93.7
	313	534	189.5	111.46	85.6
	323	500	187	267.62	78.5
	333	494	193	626.53	62.03

In order to investigate the inhibitive performance of (PT) affected by temperature, potentiodynamic polarization measurements were performed at various temperatures, ranging from 303 to 333K, with and without 1.0 mM (PT). Consequently, the activation energy (E_a), the enthalpy of activation (ΔH_a) and the entropy of activation (ΔS_a) for the corrosion of carbon steel in 1.0M HCl in the absence and presence of 1.0 mM (PT) are calculated using Arrhenius equation [56-57] and transition state equation[58-60], respectively:

$$I_{corr} = k \exp\left(-\frac{E_a}{RT}\right) \quad (7)$$

$$I_{corr} = \frac{RT}{Nh} \exp\left(\frac{\Delta S_a}{R}\right) \exp\left(\frac{\Delta H_a}{RT}\right) \quad (8)$$

Where k is the Arrhenius pre-exponential factor, T the absolute temperature, E_a the activation corrosion energy for the corrosion process, h the Planck's constant, N the Avogadro's number, ΔS_a the entropy of activation, ΔH_a the enthalpy of activation and I_{corr} is the corrosion rate.

According to the data in Table 5, the plots of $\ln I_{\text{corr}}$ versus $1/T$ (Fig. 9) and $\ln (I_{\text{corr}}/T)$ versus $1/T$ (Fig. 10) show almost straight lines and all the regression coefficients are close to 1. From the slopes and intercepts of the straight lines, the values of E_a , ΔH_a and ΔS_a were calculated and listed in Table 5.

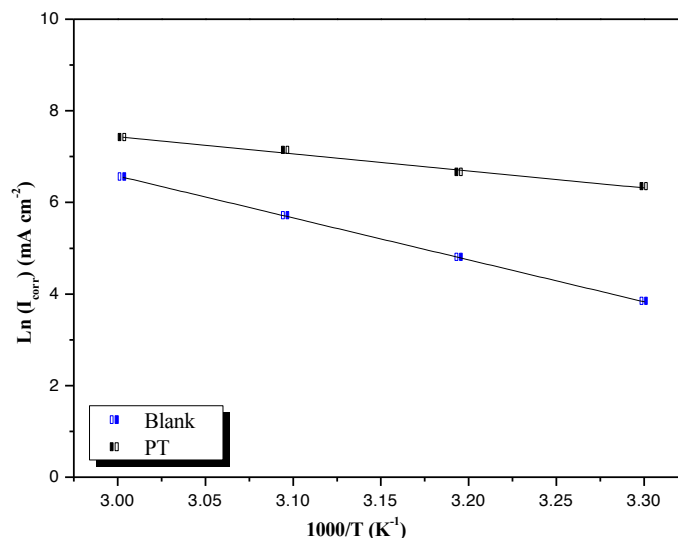


Figure 9: Arrhenius plots of carbon steel in 1.0 M HCl with and without 10^{-3} M of (PT).

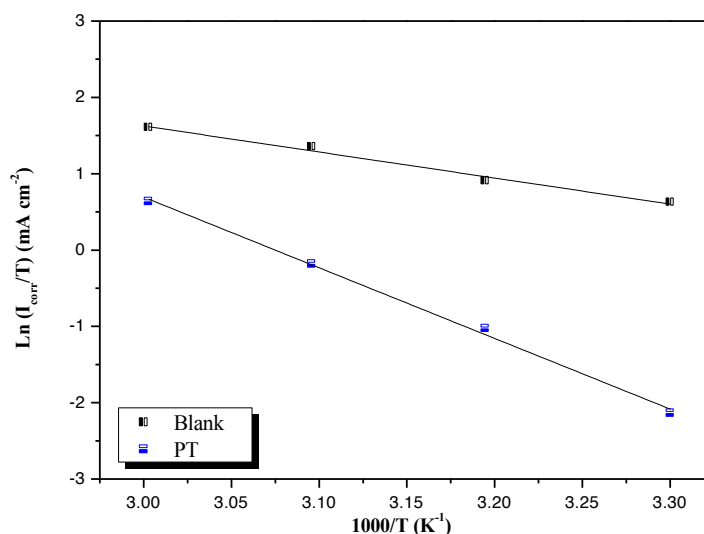


Figure 10: Relation between $\ln(I_{\text{corr}}/T)$ and $1000/T$ at different temperatures.

Inspection of Table 5 shows that the value of E_a determined in solutions containing (PT) is higher than that of in the absence of inhibitor (blank). It revealed an increase of E_a values in presence of inhibitor. For inhibitors, E_a (inhibited solution) $>$ E_a (uninhibited solution), which further confirm η (%) decreases with increase in temperature. Szauer and Brand explained that the increase in activation energy can be attributed to an appreciable decrease in the adsorption of the inhibitor on the carbon steel surface with increase in temperature. A corresponding increase in the corrosion rate occurs because of the greater area of metal that is consequently exposed to the acid environment [61].

On the other hand, the inspection of the same table revealed that the thermodynamic parameters (ΔS_a and ΔH_a) for dissolution reaction of Carbon steel in 1.0 M HCl in the presence of inhibitor are lower than that obtained in the

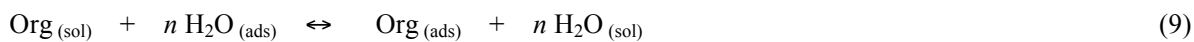
absence of inhibitor. The positive sign of ΔH_a reflects the endothermic nature of the Carbon steel dissolution process suggesting that the dissolution of Carbon steel is slow [62]. In the presence of (PT), the increase of ΔS_a reveals that an increase in disordering takes place on going from reactants to the activated complex [63].

Table 5. The value of activation parameters for carbon steel in 1.0 M HCl in the absence and presence of 10^{-3} M of (PT).

Concentration (M)	E_a (kJ mol ⁻¹)	ΔH_a (kJ mol ⁻¹)	ΔS_a (J mol ⁻¹ K ⁻¹)	$E_a - \Delta H_a$ (kJ mol ⁻¹)
Blank	31.03	28.51	-99	2.52
1×10^{-3} M	76.12	73.59	39.07	2.52

3.5. Adsorption isotherm and thermodynamic parameters

The values of surface coverage θ corresponding to different concentrations of (PT) in the temperature 298K have been used to explain the best isotherm to determine the adsorption process. The fractional surface coverage θ can be easily determined by the ratio η (%) / 100 (Table 5), if one assumes that the values of η (%) do not differ substantially from surface coverage (θ). As it is known that the adsorption of an organic adsorbate onto metal-solution interface can be presented as a substitution adsorption process between the organic molecules in the aqueous solution $Org_{(sol)}$ and the water molecules on the metallic surface $H_2O_{(ads)}$:



where $Org_{(sol)}$ and $Org_{(ads)}$ are the organic molecules in the aqueous solution and adsorbed on the metallic surface, respectively, $H_2O_{(ads)}$ is the water molecules on the metallic surface, n is the size ratio representing the number of water molecules replaced by one molecule of organic adsorbate. When the equilibrium of the process described in this equation is reached, it is possible to obtain different expressions of the adsorption isotherm plots, and thus the surface coverage degree (θ) can be plotted as a function of the concentration of the inhibitor under test [64]. The Langmuir adsorption isotherm was found to give the best description of the adsorption behaviour of (PT). In This case, the surface coverage (θ) of the inhibitor on the steel surface is related to the concentration of inhibitor in the solution according to the following equation:

$$\frac{\theta}{1 - \theta} = K_{ads} C_{inh} \quad (10)$$

Rearranging this equation gives:

$$\frac{C_{inh}}{\theta} = \frac{1}{K_{ads}} + C_{inh} \quad (11)$$

Where θ is the surface coverage degree, C_{inh} is the inhibitor concentration in the electrolyte and K_{ads} is the equilibrium constant of the adsorption process. The K_{ads} values may be taken as a measure of the strength of the adsorption forces between the inhibitor molecules and the metal surface [65]. To calculate the adsorption parameters, the straight lines were drawn using the least squares method. The experimental (points) and calculated isotherms (lines) are plotted in Fig. 8. The results are presented in Table 5. Adsorption models- Langmuir, Temkin and Frunkin isotherms were tested graphically for the data and a very good fit is observed with a regression coefficient (R^2) up to 0.99995 and the obtained lines have slopes very close to unity, which suggests that the experimental data are well described by Langmuir isotherm and exhibit single-layer adsorption characteristic [55]. This kind of isotherm involves the assumption of no interaction between the adsorbed species and the electrode surface. From the intercepts of the straight lines C_{inh}/θ – axis, the K_{ads} values were calculated and given in Table 5. As can be seen from Table 5, the higher value of K_{ads} indicates that the inhibitor is easily and strongly adsorbed on the metal surface, leading to a better inhibition performance. In our case, the strong interaction of inhibitors with mild steel can be attributed to the presence of heteroatom, such as N and S, and π -electrons in the inhibitor molecules [66].

The large value of ΔG_{ads}^0 and its negative sign (in Table 6) is usually characteristic of a strong interaction and a high efficient adsorption [67].

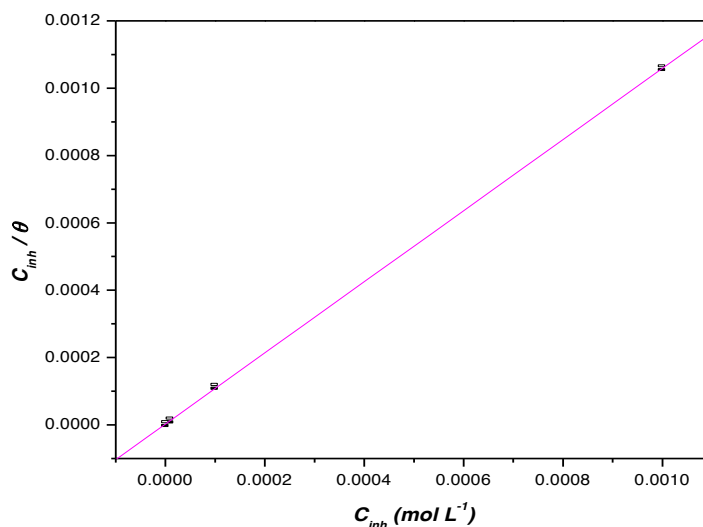


Figure 9: Langmuir's isotherm adsorption model of (PT) on the mild steel surface in 1.0 M HCl at 303K.

Table 6: Thermodynamic parameters for the adsorption of (PT) on the mild steel in 1.0 M HCl at 303K

Inh	Slope	$K_{\text{ads}} (\text{M}^{-1})$	R^2	$\Delta G_{\text{ads}}^0 (\text{kJ/mol})$
(PT)	1.05602	387229.1816	0.99995	-41.85

3.6. Theoretical parameters predicating

Computational methods have a strong impact toward the design and development of organic corrosion inhibitors. Recently, density function theory (DFT) has been used to analyze the characteristics of the inhibitor/surface mechanism and to describe the structural nature of the inhibitor on the corrosion process. Furthermore, DFT is considered to be a very useful technique to probe the inhibitor/surface interaction as well as to analyze the experimental data [68]. Thus in our present investigation, DFT method was employed to give some insight into the inhibition action of PT molecule on the carbon steel surface. The quantum chemical parameters such as E_{HOMO} , E_{LUMO} , the energy gap ΔE ($E_{\text{LUMO}} - E_{\text{HOMO}}$), and dipole moment (μ) were obtained for the neutral PT molecule to predict their activity toward metal surface. These quantum chemical parameters were generated after geometric optimization with respect to all nuclear coordinates. Figure 5 shows the optimized geometry of PT. Frontier orbital density distribution is useful in predicting adsorption centers of the PT molecule responsible for the interaction with metal surface atoms. Figure 10 shows the HOMO and the LUMO density distribution of PT.

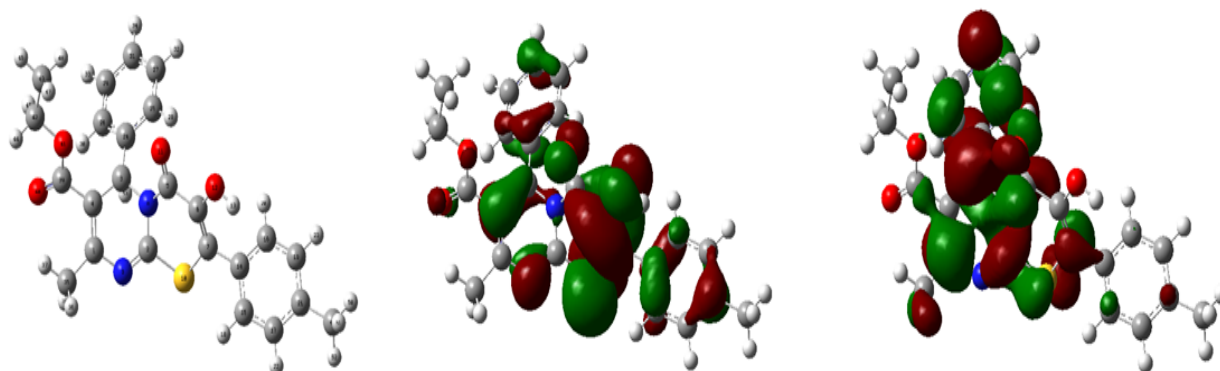


Fig. 10: Optimized structures and Frontier molecular orbital density distributions HOMO (left) and LUMO (right) of PT.

Table 7. Quantum chemical parameters for PT calculated using B3LYP/ 6-31G (d,p).

μ (debye)	TE (eV)	E_{HOMO} (eV)	E_{LUMO} (eV)	ΔE_{gap} (eV)	χ (eV)	η (eV)	ΔN
5.0273	47233.11	-4.48961	-1.74561	2.744	3.11761	1.37199	1.08625

According to frontier orbital theory, the reaction of reactants mainly occurred on the highest occupied molecular orbital (HOMO) and lowest unoccupied molecular orbital (LUMO). The energy of HOMO (E_{HOMO}) is related to ionization potential while the energy of LUMO (E_{LUMO}) is directly related to electron affinity. Higher values of E_{HOMO} indicate a tendency of the inhibitor molecules to donate electrons to appropriate acceptor molecules with low energy or empty 3d orbital of Fe to form coordinate bond [69]. The lower values of E_{LUMO} , the stronger the electron accepting ability of the inhibitor molecule, so that back-donating bond can be formed with its anti-bonding orbital.

From Table 7, the high value of dipole moment probably increases the adsorption between chemical compound and metal surface [70]. The adsorption of PT molecules from the aqueous solution can be regarded as a quasi-substitution process between the PT in the aqueous phase [PT (sol)] and water molecules at the electrode surface [H_2O (ads)].

E_{HOMO} is often associated with the electron-donating ability of a molecule and its high value (-4.48961eV) is likely to indicate a tendency to donate electrons to appropriate low-energy acceptor states. Increasing values of the E_{HOMO} facilitate adsorption (and therefore inhibition) by influencing the transport process through the adsorbed layer. E_{LUMO} indicates the ability of the molecule to accept electrons; hence these are the acceptor states. The lower the value (-1.74561eV) of E_{LUMO} , the more probable it is that the molecule would accept electrons [71]. As for the values of ΔE ($E_{\text{LUMO}} - E_{\text{HOMO}}$), lower values (2.744) of the energy difference ΔE will cause higher inhibition efficiency because the energy to release an electron from the last occupied orbital will be low [72]. The total energy of the PT is equal to 47233.11 eV. This result indicated that PT is favorably adsorbed through the active centers of adsorption. The fraction of electrons transferred ΔN from inhibitor to mild steel surface is also calculated using a theoretical χ_{Fe} and η_{Fe} values for iron of 7 eV mol⁻¹ and 0 eV mol⁻¹, respectively [73]. The ΔN values are correlated to the inhibition efficiency resulting from electron donation. According to Lukovits et al. [35], if $\Delta N < 3.6$, the inhibition efficiency increases with increasing electron-donating ability at the metal surface. In this study, the compound is the donors of electrons, and the iron surface is the acceptor. The compound is bound to the metal surface, and thus forms an inhibition adsorption layer against corrosion. In addition, the electronegativity parameter (χ) is related to the chemical potential, and higher value of χ indicates better.

Conclusion

Ethyl3-hydroxy-8-methyl-4-oxo-6-phenyl-2-(p-toly)-4,6-dihydropyrimido[2,1-b][1,3]thiazine-7-carboxylate (PT) shows excellent inhibition properties for the corrosion of C38 steel in 1.0 M HCl at 303 K, and the inhibition efficiency increases with increasing of the (PT)concentration. The inhibitor efficiencies determined by weight loss, Tafel polarisation and EIS methods are in reasonable agreement. Based on the polarisation results, the investigated (PT) can be classified as mixed inhibitor. The EIS spec-tra is described well by a relatively simple structural model having only one time constant. The calculated structural parameters show increase of the obtained R_1 values and decrease of the capacitance, C_{dl} , with (PT) concentration increase. It is suggested to attribute this to the increase of the thickness of the adsorption layer at steel surface. The η (%) of (PT) is found to decrease proportionally with increasing temperature (303–328 K) and its addition to 1.0M HCl leads to increase of apparent activation energy (E_a) of corrosion process. The corrosion process is inhibited by the adsorption of (PT) on steel surface and the adsorption of the inhibitor fits a Langmuir isotherm model at 303 K and the negative value of the $\Delta G^\circ_{\text{ads}}$ indicates that the adsorption of the (PT) molecules is a spontaneous process. The density distributions of the frontier molecular orbitals (HOMO and LUMO) indicate that the studied derivatives adsorb through the active centers S and N atoms and π electrons of the pyrimidothiazine. The better inhibition efficiency of PT can be explained on the basis of the quantum parameters of E_{HOMO} , E_{LUMO} , χ and ΔN .

References

1. Singh A. K., Quraishi M.A. Piroxicam A novel corrosion inhibitor for mild steel corrosion in HCl acid solution, *J. Mater. Environ. Sci.* 1 (2010) 101-110
2. Prajila M.J., Bincy J., Abraham J. Electroanalytical studies on the Interaction of 4-(N, N-Dimethylaminobenzilidene)-3-mercapto-6-methyl-1, 2, 4-triazin (4H)-5-one (DAMMT) with mild steel in perchloric acid, *J. Mater. Environ. Sci.* 3 (2012) 1045-1064
3. Naik U.J., Panchal V.A., Patel A.S., Shah N.K. The corrosion inhibition study of Al -Pure By p-Anisidine -N-Benzylidene Schiff base in HCl solution, *J. Mater. Environ. Sci.* 3 (2012) 935-946
4. Al Hamzi A.H., Zarrok H., Zarrouk A., Salghi R., Hammouti B., Al-Deyab S.S., Bouachrine M., Amine A., Guenoun F. The role of acridin-9(10H)-one in the inhibition of carbon steel corrosion: Thermodynamic, electrochemical and dft studies, *Int. J. Electrochem. Sci.* 8 (2013) 2586-2605
5. Zarrouk A., Hammouti B., Zarrok H., Warad I., Bouachrine M., N-containing organic compound as an effective corrosion inhibitor for copper in 2M HNO₃ : Weight loss and quantum chemical study, *Der Pharm. Chem.* 3 (2011) 263-271
6. Ben Hmamou D., Salghi R., Zarrouk A., Messali M., Zarrok H., Errami M., Hammouti B., Bazzi L., Chakir A. Inhibition of steel corrosion in hydrochloric acid solution by chamomile extract, *Der Pharm. Chem.* 4 (2012) 1496-1505
7. Ghazoui A., Benaht N., Al-Deyab S.S., Zarrouk A., Hammouti B., Ramdani M., Guenbour M. An investigation of two novel pyridazine derivatives as corrosion inhibitor for C38 Steel in 1.0 M HCl, *Int. J. Electrochem. Sci.* 8 (2013) 2272-2292
8. Zarrouk A., Zarrok H., Salghi R., Bouroumane N., Hammouti B., Al-Deyab S.S., Touzani R., The adsorption and corrosion inhibition of 2-[Bis-(3,5-dimethyl-pyrazol-1-ylmethyl)-amino]-pentanedioic acid on carbon steel corrosion in 1.0 m HCl, *Int. J. Electrochem. Sci.* 7 (2012) 10215-10232
9. Bendaha H., Zarrouk A., Aouniti A., Hammouti B., El Kadiri S., Salghi R., Touzani R., Adsorption and corrosion inhibitive properties of some tripodal pyrazolic compounds on mild steel in hydrochloric acid systems, *Phys. Chem. News* 64 (2012) 95-103.
10. Rekkab S., Zarrok H., Salghi R., Zarrouk A., Bazzi L., Hammouti B., Kabouche Z., Touzani R., Zougagh M. Green corrosion inhibitor from essential oil of eucalyptus globulus (Myrtaceae) for C38 steel in sulfuric acid solution, *J. Mater. Environ. Sci.* 3 (2012) 613-627
11. Zarrouk, Hammouti, B., Zarrok, H., Bouachrine, M., Khaled, K.F., Al-Deyab, S.S. Corrosion inhibition of copper in nitric acid solutions using a new triazole derivative, *Int. J. Electrochem. Sci.* 7 (2012) 89-105
12. Ghazoui, A., Saddik, R., Benchat, N., Guenbour, M., Hammouti, B., Al-Deyab, S.S., Zarrouk, A. Comparative study of pyridine and pyrimidine derivatives as corrosion inhibitors of C38 steel in molar HCl, *Int. J. Electrochem. Sci.* 7 (2012) 7080-7097
13. Zarrok, H., Mamari, K.A., Zarrouk, A., Salghi, R., Hammouti, B., Al-Deyab, S.S., Essassi, E.M., Bentiss, F., Oudda, H. Gravimetric and electrochemical evaluation of 1-allyl-1H-indole-2,3-dione of carbon steel corrosion in hydrochloric acid, *Int. J. Electrochem. Sci.* 7 (2012) 10338-10357.
14. Zarrok, H., Zarrouk, A., Salghi, R., Ramli, Y., Hammouti, B., Assouag, M., Essassi, E.M., Oudda, H., Taleb, M. 3,7-dimethylquinoxalin-2-(1H)-one for inhibition of acid corrosion of carbon steel, *J. Chem. Pharm. Res.* 4 (2012) 5048-5055
15. Zarrouk, A., Hammouti, B., Dafali, A., Bentiss, F. Inhibitive properties and adsorption of purpald as a corrosion inhibitor for copper in nitric acid medium, *Ind. Eng. Chem. Res.* 52 (2013) 2560-2568
16. Zarrok, H., Zarrouk, A., Salghi, R., Oudda, H., Hammouti, B., Assouag, M., Taleb, M., Ebn Touhami, M., Bouachrine, M., Boukhris, S. Gravimetric and quantum chemical studies of 1-[4-acetyl-2-(4-chlorophenyl)quinoxalin-1(4H)-yl] acetone as corrosion inhibitor for carbon steel in hydrochloric acid solution, *J. Chem. Pharm. Res.* 4 (2012) 5056-5066.
17. H. Zarrok, H. Oudda, A. El Midaoui, A. Zarrouk, B. Hammouti, M. Ebn Touhami, A. Attayibat, S. Radi, R. Touzani, Some new bipyrazole derivatives as corrosion inhibitors for C38 steel in acidic medium, *Res. Chem. Intermed.* 38 (2012) 2051-2063
18. Ghazoui, A., Zarrouk, A., Benaht, N., Salghi, R., Assouag, M., El Hezzat, M., Guenbour, A., Hammouti, B. New possibility of mild steel corrosion inhibition by organic heterocyclic compound, *J. Chem. Pharm. Res.* 6 (2014) 704-712

19. Zarrok, H., Zarrouk, A., Salghi, R., Ebn Touhami, M., Oudda, H., Hammouti, B., Touir, R., Bentiss, F., Al-Deyab, S.S. Corrosion inhibition of C38 steel in acidic medium using N-1 naphthylethylenediamine dihydrochloride monomethanolate, *Int. J. Electrochem. Sci.* 8 (2013) 6014-6032
20. Zarrouk, A., Zarrok, H., Salghi, R., Touir, R., Hammouti, B., Benchat, N., Afrine, L.L., Hannache, H., El Hezzat, M., Bouachrine, M. Electrochemical impedance spectroscopy weight loss and quantum chemical study of new pyridazine derivative as inhibitor corrosion of copper in nitric acid, *J. Chem. Pharm. Res.* 5 (2013) 1482-1491
21. Zarrok, H., Zarrouk, A., Salghi, R., Assouag, M., Hammouti, B., Oudda, H., Boukhris, S., Al Deyab, S.S., Warad, I. Inhibitive properties and thermodynamic characterization of quinoxaline: Derivative on carbon steel corrosion in acidic medium, *Der Pharm. Lett.* 5 (2013) 43-53
22. Ben Hmamou, D., Aouad, M.R., Salghi, R., Zarrouk, A., Assouag, M., Benali, O., Messali, M., Zarrok, H., Hammouti, B. Inhibition of C38 steel corrosion in hydrochloric acid solution by 4,5-Diphenyl-1H-Imidazole-2-Thiol: Gravimetric and temperature effects treatments, *J. Chem. Pharm. Res.* 4 (2012) 3498-3504.
23. Stoyanova, A.E., Peyerimhoff, S.D. On the relationship between corrosion inhibiting effect and molecular structure *Electrochim. Acta*, 47 (2002) 1365-1371
24. Valdez, L.M.R., Villafane, A.M., Mitnik, D.G. CHIH-DFT computational molecular characterization of phenanthro [9, 10-c]-1,2,5 thiadiazole 1,1-dioxide, *J. Mol. Struct. Theochem.* 716 (2005) 61-65
25. B. Gomez, N.V. Likhanova, M.A.D. Aguilar, R.M. Palou, A. Vela, J.L. Gazquez. Quantum chemical study of the inhibitive properties of 2-pyridyl-azoles, *J. Phys. Chem. B.* 18 (2006) 8928–8934
26. M. Finšgar, A. Lesar, A. Kokalj, I. Milošev. A comparative electrochemical and quantum chemical calculation study of BTAH and BTAOH as copper corrosion inhibitors in near neutral chloride solution, *Electrochim. Acta*, 53 (2008) 8287-8297
27. Serrar, H., Boukhris, S., Hassikou, A., Souizi, A. Efficient and easy one-pot synthesis of new 3,5-dioxo-thiazolo[2,3-a] pyrimidine-6- carbonitrile and 4,6- dioxo- pyrimido[2,1- b][1,3]thia zine-7- carbonitrile derivatives, *J. Heterocyclic Chem.*, (2013) DOI 10.1002/jhet.2085
28. A. D, Becke Density-Functional Thermochemistry. I. The Effect of the Exchange-Only Gradient Correction, *J. Chem. Phys.* 96, (1992) 2155–2160
29. A.D. Becke New mixing of Hartree-Fock and local density-functional theories *J. Chem. Phys.*, 98, (1993) 1372
30. C. Lee, W. Yang, R.G. Parr, Development of the Colle-Salvetti correlation-energy formula into a functional of the electron density, *Phys. Rev. B* 37 (1988) 785–789.
31. M.J. Frisch et al., GAUSSIAN 03, Revision B.03, Gaussian, Inc., Wallingford, CT, 2004.
32. M.J.S. Dewar, W. Thiel, "Ground States of Molecules. 38. The MNDO Method. Approximations and Parameters.", *J. Am. Chem. Soc.*, 99 (1977) 4899.
33. R.G. Pearson, Absolute electronegativity and hardness: application to inorganic chemistry, *Inorg. Chem.* 27 (1988) 734–740.
34. V.S. Sastri, J.R. Perumareddi, Molecular orbital theoretical studies of some organic corrosion inhibitors, *Corrosion* 53 (1997) 671–678.
35. I. Lukovits, E. Kalman and F. Zucchi, "Corrosion Inhibitors—Correlation between Electronic Structure and Efficiency," *Corrosion*, 57 (2001) 3-8.
36. Lebrini, M., Bentiss, F., Chihib, N., Jama, C., Hornez, J. P., Lagrenée, M. Polyphosphate derivatives of guanidine and urea copolymer: Inhibiting corrosion effect of armco iron in acid solution and antibacterial activity, *Corros. Sci.* 50 (2008) 2914-2918
37. McCafferty E. Validation of corrosion rates measured by the Tafel extrapolation method, *Corros. Sci.* 47 (2005) 3202-3215
38. Bouklah M., Benchat N., Aouniti A., Hammouti B., Benkaddour M., Lagrenée M., Vezin H., Bentiss F., *Prog. Org. Coat.* 51 (2004) 118-124
39. Bentiss F., Jama C., Mernari B., El Attari H., El Kadi L., Lebrini M., Traisnel M., Lagrenée M. Corrosion control of mild steel using 3,5-bis(4-methoxyphenyl)-4-amino-1,2,4-triazole in normal hydrochloric acid medium, *Corros. Sci.* 51 (2009) 1628-1635

40. Ferreira, E.S., Giancomelli, C., Giacomelli, F.C., Spinelli, A. Evaluation of the inhibitor effect of L-ascorbic acid on the corrosion of mild steel, *Mater. Chem. Phys.* 83 (2004) 129-134
41. Singh, A. K., Quraishi, M. A. Inhibitive effect of diethylcarbamazine on the corrosion of mild steel in hydrochloric acid *Corros. Sci.* 52 (2010) 1529-1535
42. Abdel-Gaber, A.M., Abd-El-Nabey, B.A., Sidahmed, I.M., El-Zayady, A.M., Saadawy, M. Inhibitive action of some plant extracts on the corrosion of steel in acidic media, *Corros. Sci.* 48 (2006) 2765-2779
43. Macdonald, J.R., Johanson W.B. Theory in Impedance Spectroscopy, John Wiley & Sons, New York, J.R. Macdonald (Ed.) (1987)
44. Abdelaal, M.S., Morad, M.S. Inhibiting effects of some quinolines and organic phosphonium compounds on corrosion of mild steel in 3M HCl solution and their adsorption characteristics, *Br. Corros. J.* 36 (2001) 253-260
45. Bommersbach, P., Alemany-Dumont, C., Millet, J.P., Normand B. Formation and behaviour study of an environment-friendly corrosion inhibitor by electrochemical methods, *Electrochim. Acta* 51 (2005) 1076-1084
46. Mansfeld, F. Recording an analysis of AC impedance data for corrosion studies, *Corrosion.* 36 (1981) 301-307
47. Benedetti, A.V., Sumodjo, P.T.A., Nobe, K., Cabot, P.L., Proud, W.G. Electrochemical studies of copper, copper-aluminium and copper-aluminium-silver alloys: Impedance results in 0.5M NaCl, *Electrochim. Acta* 40 (1995) 2657-2668
48. Satapathy, A.K., Gunasekaran, G., Sahoo, S.C., Amit, K., Rodrigues, P.V. Corrosion inhibition by Justicia gendarussa plant extract in hydrochloric acid solution, *Corros. Sci.* 51 (2009) 2848-2856
49. Emregul, K.C., Atakol, O. Corrosion inhibition of iron in 1 M HCl solution with Schiff base compounds and derivatives, *Mater. Chem. Phys.* 83 (2004) 373-379
50. Rosenfield, I.L. Corrosion Inhibitors Fundamental Aspects of Corrosion Films in Corrosion Science, McGraw-Hill, New York, 5 (1981) 301-307
51. MaCafferty, M., Hackerman, N. Double Layer Capacitance of Iron and Corrosion Inhibition with Polymethylene Diamines, *J. Electrochim. Soc.* 119 (1972) 146-154
52. Hosseini, M., Mertens, S.F.L., Ghorbani, M., Arshadi, R.M. Asymmetrical Schiff bases as inhibitors of mild steel corrosion in sulphuric acid media, *Mater. Chem. Phys.* 78 (2003) 800-808
53. Chen, W., Luo, H.Q., Li, N.B. Inhibition effects of 2, 5-dimercapto-1, 3, 4-thiadiazole on the corrosion of mild steel in sulphuric acid solution, *Corros. Sci.* 53 (2011) 3356-3365
54. Abd El-Rehim, S.S., Ibrahim, M.A.M., Khaled, K.F. 4-Aminoantipyrine as an inhibitor of mild steel corrosion in HCl solution, *J. Appl. Electrochem.* 29 (1999) 593 -599
55. Bentiss, F., Lebrini, M., Lagrenée, M. Thermodynamic characterization of metal dissolution and inhibitor adsorption processes in mild steel/2,5-bis(*n*-thienyl)-1,3,4-thiadiazoles/hydrochloric acid system, *Corros. Sci.* 47 (2005) 2915-2931
56. Xu B, Liu Y, Yin X S, Yang W Z, Chen Y Z. Experimental and theoretical study of corrosion inhibition of 3-pyridine carboxaldehyde thiosemicarbazone for mild steel in hydrochloric acid, *Corros. Sci.* 74 (2013) 206-213
57. Yang, Xu B., Liu, W Z., Yin, Y., Gong, X S., Chen, Y Z. Experimental and theoretical evaluation of two pyridine carboxaldehyde thiosemicarbazone compounds as corrosion inhibitors for mild steel in hydrochloric acid solution. *Corros. Sci.* 78 (2014) 260-268
58. Zheng, X W., Zhang, S T., Li, W P., Yin, L L., He, J H., Wu, J F. Investigation of 1-butyl-3-methyl-1H-benzimidazolium iodide as inhibitor for mild steel in sulfuric acid solution. *Corros. Sci.* 80 (2014) 383-92
59. Hegazy, M A., El Tabei, A S., Bedai, A H., Sadeq, M A. An investigation of three novel non ionic surfactants as corrosion inhibitor for carbon steel in 0.5 M H₂SO₄. *Corros. Sci.* 54 (2012) 219-230
60. Yadav, D K., Quraishi, M A., Maiti, B. Inhibition effect of some benzylidenes on mild steel in 1 M HCl: An experimental and theoretical correlation. *Corros. Sci.* 55 (2012) 254-266
61. Szauer T., Brandt A. Adsorption of oleates of various amines on iron in acidic solution, *Electrochim. Acta* 26 (1981) 1253-1256
62. Guan N. M., Xueming L., Fei L. Synergistic inhibition between o-phenanthroline and chloride ion on cold rolled steel corrosion in phosphoric acid *Mater. Chem. Phys.* 86 (2004) 59-68
63. Khamis E., Hosney A., El-Khodary S., *Afinidad*, 52(1995) 95.

64. Labjar N., Bentiss F., Lebrini M., Jama C., El hajjaji S., Study of Temperature Effect on the Corrosion Inhibition of C38 Carbon Steel Using Amino-tris(Methylenephosphonic) Acid in Hydrochloric Acid Solution, *Inter. J. Corros.* (2011) 528-548
65. Amin M.A., Study of Temperature Effect on the Corrosion Inhibition of C38 Carbon Steel Using Amino-tris(Methylenephosphonic) Acid in Hydrochloric Acid Solution, *J. Appl. Electrochem.* 36 (2006) 215-226
66. Özkır D., Kayakırılmaz K., Bayol E., Gürten A.A., Kandemirli F., The inhibition effect of Azure A on mildsteel in 1 M HCl. A complete study: Adsorption, temperature, duration and quantum chemical aspects, *Corros. Sci.* 56 (2012) 143-152.
67. Tourabi, K., Nohair, K., Nyassi, N., Hammouti, B., Bentiss, F., Chetouani, A. Mor. Enhancement of corrosion protection efficiency of mild steel by 3,5-di(4-tolyl)-4-amino-1,2,4-triazole in hydrochloric acid medium, *J. Chem.* 1 (2013) 47-54
68. Guadalupe H.J., E. Garcia-Ochoa, P.J. Maldonado-Rivas, J. Cruz, T. Pandiyan, A combined electrochemical and theoretical study of *N,N'*-bis(benzimidazole-2yl-ethyl)-1,2-diaminoethane as a new corrosion inhibitor for carbon steel surface *J. Electroanal. Chem.*, 655 (2011) 164-172.
69. Obot I.B., N.O. Obi-Egbedi, Indeno-1-one [2,3-b]quinoxaline as an effective inhibitor for the corrosion of mild steel in 0.5 M H₂SO₄ solution *Mater. Chem. Phys.*, 122(2010) 325-328.
70. Vijayakumar S., P. Kolandaivel, Study of Static dipole polarizabilities, Dipole moments, and Chemical hardness for linear CH₃- (C? C) n-X (X=H, F, Cl, Br, and NO₂ and n=1-4) molecules, *J. Mol...Struct.*, 770 (2006)23-29.
71. Gece G., The use of quantum chemical methods in corrosion inhibitor studies, *Corros. Sci.*, 50, (2008)2981-2992.
72. Issa R.M., M.K. Awad, and F.M. Atlam, Quantum Chemical Studies on the Inhibition of Corrosion of Copper Surface by Substituted Uracils, *Appl. Surf. Sci.*, 255 (2008)2433-2441.
73. Obot I.B., Obi-Egbedi N.O., Theoretical study of benzimidazole and its derivatives and their potential activity as corrosion inhibitors, *Corros. Sci.*, 52 (2010) 657-660.

(2015) ; <http://www.jmaterenvironsci.com>